Time-Resolved Investigations of Stimulated Brillouin Scattering in Transparent and Absorbing Media: Determination of Phonon Lifetimes

D. POHL* AND W. KAISER
Physik-Department der Technischen Hochschule München, Germany
(Received 8 July 1969)

Stimulated Brillouin scattering was studied both theoretically and experimentally. The evolution in time of the scattering process, its dependence on frequency, and the influence of optical absorption were analyzed. For quantitative investigations, the individual shapes of the laser and signal pulses were taken into account. Strong transient effects predicted by theory were confirmed experimentally. The amplification of Brillouin light was measured in a generator-amplifier system using single-mode giant laser pulses. Several liquids, glasses, and quartz were investigated. The experimental results allow the determination of phonon lifetimes τ and of elasto-optic constants. In our amplifier system, accurate values of τ are obtained for $\tau<3$ nsec, i.e., for liquids and some solids. The limitation of the method is discussed. In absorbing media, stimulated thermal Brillouin scattering was observed in quantitative agreement with theory.

I. INTRODUCTION

In recent years the scattering of light on density fluctuations of liquids and solids has received considerable attention. In isotropic media, the frequency spectrum of the scattered radiation consists of the central Rayleigh line and of two Brillouin lines which are Stokes and anti-Stokes shifted from the frequency ω_L of the incident radiation by an amount

$$\omega_B=(2nv\omega_L/c)\sin\tfrac{1}{2}\theta, \quad (1)$$

where n is the refractive index, v is the sound velocity of the scattering medium, c is the velocity of light, and θ is the angle between the incident and scattered wave vector. The classical Brillouin lines have, to a good approximation, a Lorentzian frequency profile; the full width at half of the intensity maximum Γ_B is a direct measure of the lifetime τ of the phonon under investigation

$$\Gamma_B=1/\tau. \quad (2)$$

According to (1) and (2), measurements of Brillouin scattering provide two important material parameters: the velocity and the lifetime of phonons at hypersonic frequencies.

The intensity of the spontaneously scattered radiation is rather weak (approximately 10^{-5}/cm rad in liquids) requiring sensitive detection systems. On the other hand, at high incident light intensities (laser giant pulses) highly amplified Brillouin radiation is observed which approaches the power level of the incoming light. In the stimulated Brillouin scattering process, the electromagnetic field produces intense density fluctuations in two ways: through electrostriction and, in absorbing media, through absorptive heating. Density fluctuations lead to changes of the index of refraction which in turn influence the propagation of the light waves.

There is an extensive theoretical[1–5] and experimental[6–10] literature dealing with the steady-state[11] problem of stimulated Brillouin scattering (SBS). Most previous investigations were made with time-integrating photocells or photographic plates (in conjunction with high-resolution spectrometers). Recent investigations using photodetectors with high time resolution gave detailed information concerning the saturation region in a traveling-wave system.[8]

In this paper, the light amplification by SBS in a generator-amplifier system is investigated theoretically and experimentally. It has been shown in recent years that several stimulated scattering phenomena are studied conveniently in an amplifier system, for example, stimulated Raman scattering,[12] SBS,[10,13] and

* Present address: IBM Zürich Research Laboratory, CH 8803 Rüschlikon, Switzerland.

[1] Y. R. Shen and N. Bloembergen, Phys. Rev. **137**, A1787 (1965).

[2] C. L. Tang, J. Appl. Phys. **37**, 2945 (1966); F. Barocchi, *ibid.* **40**, 178 (1969).

[3] D. L. Bobroff, J. Appl. Phys. **36**, 1760 (1965).

[4] N. Bloembergen and Y. R. Shen, in *Physics of Quantum Electronics*, edited by P. L. Kelley, B. Lax, and P. E. Tannenwald (McGraw-Hill Book Co., New York, 1966), p. 119 ff.

[5] K. Grob, Z. Physik **201**, 59 (1967).

[6] R. J. Chiao, C. H. Townes, and B. P. Stoicheff, Phys. Rev. Letters **12**, 592 (1964); W. Heinicke and G. Winterling, Appl. Phys. Letters **11**, 231 (1967); A. I. Ritus and A. A. Manenkov, Zh. Eksperim. i Teor. Fiz. Pis'ma v Redaktsiyu **6**, 927 (1967) [English transl.: Soviet Phys.—JETP Letters **6**, 349 (1967)]; P. Asam, P. Deuflhard, and W. Kaiser, Phys. Letters **27A**, 78 (1968).

[7] E. Garmire and C. H. Townes, Appl. Phys. Letters **5**, 84 (1964); R. G. Brewer, *ibid.* **5**, 127 (1964); R. G. Brewer and K. E. Riekhoff, Phys. Rev. Letters **13**, 334 (1964); A. S. Pine, Phys. Rev. **149**, 113 (1966); M. Maier, W. Rother, and W. Kaiser, Phys. Letters **23**, 83 (1966); T. A. Wiggins, R. B. Wick, N. D. Foltz, C. W. Cho, and D. H. Rank, J. Opt. Soc. Am. **57**, 661 (1967); J. Walder and C. L. Tang, Phys. Rev. Letters **19**, 623 (1967); D. Pohl, Phys. Letters **24A**, 239 (1967); Y. R. Shen and Y. J. Shahan, Phys. Rev. **163**, 224 (1967); S. L. Shapiro, J. A. Giordmaine, and K. W. Wecht, Phys. Rev. Letters **19**, 1093 (1967); I. L. Fabelinskii and V. S. Starunov, Appl. Opt. **6**, 1793 (1967); G. Winterling, G. Walda, and W. Heinicke, Phys. Letters **26A**, 301 (1968); M. Maier, W. Rother, and W. Kaiser, Appl. Phys. Letters **10**, 80 (1967).

[8] M. Maier, Phys. Rev. **166**, 113 (1968).

[9] E. E. Hagenlocker and W. G. Rado, Appl. Phys. Letters **7**, 236 (1965); E. E. Hagenlocker, R. W. Minck, and G. Rado, Phys. Rev. **154**, 226 (1967).

[10] M. Denariez and G. Bret, Phys. Rev. **171**, 160 (1968).

[11] More accurately one should speak of a quasi-steady-state in experimental investigations, since the phenomenon lasts only approximately 20 nsec, the duration of the light pulses (cf. Sec. II B).

[12] N. Bloembergen, G. Bret, P. Lallemand, A. Pine, and P. Simova, IEEE J. Quantum Electron. **3**, 197 (1967).

[13] D. Pohl, M. Maier, and W. Kaiser, Phys. Rev. Letters **20**, 366 (1968).

stimulated Rayleigh-wing scattering,[10] stimulated thermal Brillouin,[14] and thermal Rayleigh scattering[15] were investigated by this technique. Our amplifier system[13] has a series of advantages which make it most suitable for a quantitative analysis. (i) The amplification was investigated as a function of time, making transient and steady-state phenomena readily observable. (ii) During each pulse the amplification was determined as a function of the instantaneous laser and signal intensity allowing a direct calculation of the gain factor g. (iii) The incoming signal was tailor-made in magnitude and shape. (iv) Well-defined frequency differences between generator and amplifier were introduced. (v) The lengths of the amplifier cell and the light intensities were chosen small enough to avoid the occurrence of other competing nonlinear processes such as stimulated thermal Rayleigh scattering, stimulated Raman scattering, self-focusing, or self-trapping.

In Sec. II, the theory of a small-signal Brillouin amplifier is developed with special emphasis on the transient situation. The influence of finite light pulses on the gain factor and on the determination of phonon lifetimes is analyzed. In Sec. III, our experimental system is briefly discussed. Section IV contains the various experimental results and a detailed comparison with theory.

II. THEORY OF SBS IN TRANSPARENT AND ABSORBING MEDIA

The theory of SBS in transparent media[1–5,16] has been discussed repeatedly in the literature. The effect of absorption on SBS was recently pointed out by Herman and Gray.[17] Most of the theoretical work was concerned with the steady-state situation only. It has been found, however, that transient effects are of significance in many experimental situations.[9,13,15,15a] We wish to extend the existing theory to include the transient behavior of Brillouin amplifiers.

In the first part of this section we derive an equation for the Stokes-shifted Brillouin intensity which allows a ready application to steady-state and transient situations. We start with the nonlinear wave equation for the total electromagnetic field $\mathbf{E}$:

$$\frac{\partial^2}{\partial t^2}\mathbf{E}+\frac{\alpha c}{n}\frac{\partial}{\partial t}\mathbf{E}-\left(\frac{c}{n}\right)^2\nabla^2\mathbf{E}=\frac{\gamma^e}{n^2\rho}\frac{\partial^2}{\partial t^2}(\mathbf{E}\bar{\rho}). \tag{3}$$

The right-hand side represents the nonlinear driving term in the presence of density fluctuations. The linear optical absorption coefficient of the medium is denoted by α, and γ^e is the elasto-optic coupling parameter which is related to the Pockel's constant p by

$$\gamma^e=n^4p. \tag{4a}$$

In this paper, we consider mostly longitudinal waves in isotropic media, where the photoelastic tensor $p_{ij}(i,j=1\cdots6)$ reduces to a single component p. Using the definition $p=(\rho_0/\epsilon^2)(\partial\epsilon/\partial\rho)_T$ we obtain to a good approximation for liquids

$$\gamma^e=\tfrac{1}{3}(n^2-1)(n^2+2). \tag{4b}$$

In (3) a small additional coupling term[18] involving $(\partial\epsilon/\partial T)_\rho$ has been omitted.

We now turn to the discussion of the linearized hydrodynamic equations. Following Herman and Gray[17] and Mountain,[19] we write for the density and temperature variation under the influence of electromagnetic waves:

Equation of continuity

$$\frac{\partial\bar{\rho}}{\partial t}+\rho_0\,\mathrm{div}\mathbf{V}=0, \tag{5}$$

Navier-Stokes equation

$$\rho_0\frac{\partial\mathbf{V}}{\partial t}+\frac{v^2}{\gamma}\nabla\bar{\rho}+\frac{v^2\beta\rho_0}{\gamma}\nabla\bar{T}-\eta\nabla^2\mathbf{V}=\frac{\gamma^e}{8\pi}\nabla^2\mathbf{E}^2, \tag{6}$$

energy-transport equation

$$\rho_0c_v\frac{\partial\bar{T}}{\partial t}-\lambda\nabla^2\bar{T}-\frac{c_v(\gamma-1)}{\beta}\frac{\partial\bar{\rho}}{\partial t}=\frac{nc\alpha}{4\pi}\mathbf{E}^2. \tag{7}$$

In (6) a term representing the electrostrictive force $(\gamma^e/8\pi)\nabla^2\mathbf{E}^2$ was added to the equation of motion, and in (7) absorptive heating in the form $(nc\alpha/4\pi)\mathbf{E}^2$ was added as a heat source. The various symbols in (5)–(7) are defined as follows: $\mathbf{V}$ is the velocity of the mass element; $\gamma=c_p/c_v$ is the ratio of the specific heats; λ and β are the coefficients of heat conduction and thermal expansion, respectively; η is a constant which characterizes the damping of the acoustic wave. In liquids, η is written, to a good approximation, in the form $\eta=\frac{4}{3}\eta_S+\eta_B$, where η_S is the shear viscosity, and η_B is the "bulk" viscosity which is connected to the relaxation processes between the internal and external degrees of freedom of the molecules. η is directly related to the phonon lifetime. [See Eq. (18).] Equations (5)–(7) also hold for isotropic solids; η represents again the losses of the medium.

In this paper, we investigate the amplification of a small-signal wave $\mathbf{E}_S(z,t)$ in the presence of an intense pumping field $\mathbf{E}_L(z,t)$. The two waves have the same polarization and travel into $-z$ and $+z$ directions, respectively. In the plane-wave approximation we write

[14] D. Pohl, I. Reinhold, and W. Kaiser, Phys. Rev. Letters **20**, 1141 (1968).
[15] W. Rother, D. Pohl, and W. Kaiser, Phys. Rev. Letters **22**, 915 (1969).
[15a] D. Pohl, Phys. Rev. Letters **23**, 711 (1968).
[16] N. M. Kroll, J. Appl. Phys. **36**, 34 (1965).
[17] R. M. Herman and M. A. Gray, Phys. Rev. Letters **19**, 824 (1967).
[18] H. Z. Cummins and R. W. Gammon, J. Chem. Phys. **44**, 2785 (1966); I. P. Batra and R. H. Enns, Phys. Rev. (to be published).
[19] R. D. Mountain, Rev. Mod. Phys. **38**, 205 (1966).

(dropping the vectorial signs on the right-hand side)

$$\mathbf{E}_L(z,t)=\tfrac{1}{2}[E_L(z,t)\exp(i\omega_L t-ik_L z-\tfrac{1}{2}\alpha z)+\text{c.c.}] \quad (8)$$

and

$$\mathbf{E}_S(z,t)=\tfrac{1}{2}[E_S(z,t)\exp(i\omega_s t+ik_s z+\tfrac{1}{2}\alpha z)+\text{c.c.}]. \quad (9)$$

The linear absorption coefficient α is taken into account explicitly making E_L and E_S independent of α. The stimulated density and temperature waves have the form

$$\tilde{\rho}(z,t)=\tfrac{1}{2}[\rho(z,t)\exp(i\omega t-ikz)+\text{c.c.}], \quad (10)$$

$$\tilde{T}(z,t)=\tfrac{1}{2}[T(z,t)\exp(i\omega t-ikz)+\text{c.c.}]. \quad (11)$$

They travel in the $+z$ direction, with a frequency and a wave vector given by

$$\omega=\omega_L-\omega_S\simeq\omega_B, \quad (12a)$$

$$k=k_L+k_S\simeq k_B\simeq 2k_L, \quad (12b)$$

where ω_B is the Brillouin shift defined by (1), and k_B is given by the relation

$$k_B=\omega_B/v. \quad (13)$$

A small-signal theory will be presented here with negligible change of the pumping field, i.e., $\partial E_L/\partial z\ll E_L/l$, where l is the length of the amplifier. It will be seen in the experimental part of this paper that the slowly varying envelope approximation holds well for our investigations, i.e., we write

$$\left|\frac{1}{\omega_S}\frac{\partial E_S}{\partial t}\right| \text{ and } \left|\frac{1}{k_S}\frac{\partial E_S}{\partial z}\right|\ll E_S, \text{etc.} \quad (14)$$

Eliminating $\mathbf{V}$ from (5) and (6), and introducing (8)–(11) into (3), (6), and (7), we obtain a system of ordinary linear differential equations for the amplitudes E_S, ρ, and T:

$$\left(\frac{k^2v^2}{\gamma}-\omega^2+i\omega\Gamma_B+2(i\omega+\Gamma_B)\frac{d}{dt}+\frac{d^2}{dt^2}\right)\rho(z,t)$$
$$+\frac{k^2v^2\beta\rho_0}{\gamma}T(z,t)=\frac{\gamma^e k^2}{8\pi}E_L(t)E_S^*(z,t), \quad (15)$$

$$-(\gamma-1)\left(i\omega+\frac{d}{dt}\right)\rho(z,t)+\beta\rho_0\left(i\omega+\tfrac{1}{2}\gamma\Gamma_R+\frac{d}{dt}\right)T(z,t)$$
$$=\frac{\gamma\gamma^a k}{8\pi v}E_L(t)E_S^*(z,t), \quad (16)$$

$$\frac{d}{dz}E_S(z,t)=-i\frac{\gamma^e\omega_s}{4nc\rho_0}E_L(t)\rho^*(z,t)e^{-\alpha z/2}. \quad (17)$$

In (13)–(15), the abbreviations (18)–(20) were introduced:

$$\Gamma_B=\eta k^2/\rho_0. \quad (18)$$

As pointed out in the Introduction, Γ_B represents the damping of the acoustic waves; it is related to the phonon lifetime by (2). Similarly, the decay constant of the isobaric density fluctuation is denoted by Γ_R:

$$\Gamma_R=2\lambda k^2/\rho_0 c_p, \quad (19)$$

where Γ_R is the half-width of the classical Rayleigh line. In general, the Rayleigh line is narrower than the Brillouin line and smaller than the frequency interval ω considered here; i.e., $\Gamma_R<\Gamma_B$ and $\Gamma_R\ll\omega_B$; Γ_R will be neglected in most of the following calculations. The abbreviation

$$\gamma^a=vc^2\alpha\beta/c_p\omega_L=2nv^2c\alpha\beta/c_p\omega_B \quad (20)$$

is called the thermo-optic coupling coefficient.

Equations (15) and (16) describe the reaction of a density and temperature wave of frequency ω to a disturbance by an electric field $E_LE_S^*$ of approximately the same frequency. On the other hand, the reaction of the signal field E_S on the periodic disturbance $E_L\rho^*$ is determined by (17). The simple form of (17) allows an immediate integration. Without restricting the generality we assume E_L and $E_S(0,t)$ to be real. Using the relation $I_L=(nc/8\pi)|E_L(z,t)|^2e^{-\alpha z}$ and an equivalent expression for I_S, we transform (17) into an equation for intensities. Considering the fact that we work with small signals and small amplification, we obtain

$$I_S(z,t)=I_S(0,t)e^{\alpha z}\left\{1-[I_L(t)/I_S(0,t)]^{1/2}(\gamma^e\omega_s/2nc\rho_0)\right.$$
$$\left.\times\int_0^z e^{-\alpha z'/2}\,\mathrm{Im}\rho(z',t)\,dz'\right\}. \quad (21)$$

The first factor on the right-hand side represents the linear loss of the incident signal (note that the signal travels in the $-z$ direction) while the curly brackets describe the amplification of the signal. It should be noted that the amplification is determined by the component of the sound wave which is out of phase by $\frac{1}{2}\pi$ with $E_LE_S^*$.

We now turn to the discussion of some special cases.

A. Steady-State Solutions

Neglecting all the time derivatives in (15) and (16), we obtain the steady-state density variation ρ_{st}:

$$\rho_{st}(z)=\frac{E_LE_S^*(z)}{16\pi}\frac{\omega_B}{v^2}\frac{-\gamma^a+i\gamma^e}{\Delta\omega+\frac{1}{2}i\Gamma_B}. \quad (22)$$

Introducing (22) in (17) and going again to intensities we obtain for the signal wave at frequencies close to ω_B:

$$\frac{dI_S}{dz}=I_S[-gI_L\exp(-\tfrac{1}{2}\alpha z)+\alpha]; \quad (23)$$

for $\frac{1}{2}\alpha z\ll 1$:

$$I_S(z)=I_S(0)\exp(-gI_Lz+\alpha z), \quad (24)$$

where

$$g=g(\Delta\omega,\infty)=\frac{\gamma^e\omega_S{}^2}{nc^3\rho_0 v}\frac{\frac{1}{2}\gamma^e\Gamma_B+\gamma^a\Delta\omega}{\Delta\omega^2+(\frac{1}{2}\Gamma_B)^2} \tag{25}$$

is the frequency-dependent gain factor for the steady-state amplification process. Here

$$\Delta\omega=\omega-\omega_B \tag{26}$$

has been introduced, which represents a small deviation from the Brillouin frequency ω_B. It is seen from (25) that the total gain is the sum of two components:

(i) The first term gives the steady-state gain of SBS in transparent media which has been derived in a number of previous publications.[1-5] The same Lorentzian frequency profile is found in the classical Brillouin scattering. In measuring the gain coefficient as a function of $\Delta\omega$, the width at half-maximum gain, Γ_B is obtained. In most experimental situations, however, the steady state is not completely attained and corrections have to be introduced (see below).

For $\Delta\omega=0$ (frequency match between oscillator and amplifier), we obtain the maximum gain

$$g_{\max}{}^e=(\gamma^e\omega_L)^2/(nc^3\rho_0 v\Gamma_B)=g(\infty)=A2\tau. \tag{27}$$

Since $g_{\max}{}^e$ depends upon Γ_B, the knowledge of the gain maximum allows a direct calculation of the phonon lifetime; i.e., a single gain measurement provides us with a value of τ, using (24), (27), and (2).

The letter A introduced in (27) contains all the photoelastic constants relevant for the gain factor except of the phonon lifetime. A is a determining parameter in the transient theory discussed below.

(ii) The second contribution to the gain factor is caused by the linear absorption of light and by the resulting heating of the medium.[17] This term is asymmetric around the Brillouin frequency. For $\Delta\omega>0$ (Stokes side) the gain coefficient increases with the absorption coefficient of the medium. At $\Delta\omega=\frac{1}{2}\Gamma_B$ one obtains the maximum gain

$$g_{\max}{}^a=\gamma^e\gamma^a\omega_L{}^2/2nc^3\rho_0 v\Gamma_B. \tag{28}$$

The value of $g_{\max}{}^a$ is of the same order of magnitude as $g_{\max}{}^e$ for absorption coefficients of approximately $\alpha=1$ cm^{-1}. For $\Delta\omega<0$, the second term in (25) is negative, i.e., the total gain is diminished or might even be negative. In the latter case, signal light is converted back into pump light. The effect of absorptive heating on the Brillouin gain was found experimentally for the first time by the authors[14] and will be discussed in detail in Sec. IV E.

B. Transient Solutions

Transient solutions are of significance in SBS when the phonon lifetime is longer than or similar to the pulse length of the signal and pump light. A previous investigation by Kroll[16] of the transient behavior of SBS led to complicated integral equations which cannot readily be compared with our experimental data.

We study the transient behavior of a Brillouin light amplifier by starting from (15) to (17). In the small-amplification approximation the amplitudes of E_S, ρ, and T may be written in power series of the form

$$\rho(z,t)=\rho^0(t)+\rho^1(t)z/l+\cdots, \tag{29a}$$

$$T(z,t)=T^0(t)+T^1(t)z/l+\cdots, \tag{29b}$$

$$E_S(z,t)=E_S{}^0(t)+E_S{}^1(t)z/l+\cdots, \tag{29c}$$

while E_L is assumed to be independent of z. $E_S{}^0(t)$ represents the input signal at $z=0$ and $E_S{}^1(t)$ the first-order increase of the signal due to SBS. Introducing (29a) and (29b) into (15)–(17), and comparing the coefficients belonging to the same powers of z, a set of ordinary linear inhomogeneous differential equations is obtained. The lowest-order equations are

$$\left[\left(\frac{\omega_B{}^2}{\gamma}-\omega^2+i\omega\Gamma_B\right)+(2i\omega+\Gamma_B)\frac{d}{dt}+\frac{d^2}{dt^2}\right]\rho^0(t)+\frac{\omega_B{}^2\beta\rho_0}{\gamma}T^0(t)=\frac{\gamma^e k^2}{8\pi}E_L(t)E_S{}^{0*}(t), \tag{30}$$

$$-(\gamma-1)\left(i\omega+\frac{d}{dt}\right)\rho^0(t)+\beta\rho_0\left(i\omega+\tfrac{1}{2}\gamma\Gamma_R+\frac{d}{dt}\right)T^0(t)=\frac{\gamma\gamma^a k}{8\pi v}E_L(t)E_S{}^{0*}(t), \tag{31}$$

and

$$E_S{}^1(t)=-(i\gamma^e\omega_S l/4nc\rho_0)E_L(t)\rho^{0*}(t)e^{-\alpha z/2}. \tag{32}$$

This system will be solved for the coefficient $E_S{}^1(t)$; if necessary, higher-order coefficients may be calculated.[20] We restrict our discussion to small amplification. Comparing (29c) with an exponential gain equation (for intensities) we define a time-dependent gain factor

$$g(\Delta\omega,t)=2\,\mathrm{Re}[E_S{}^1(t)/I_L(t)E_S{}^0(t)l]. \tag{33}$$

Together with (32), we obtain

$$g(\Delta\omega,t)=(\gamma^e\omega_S/2nc\rho_0)\,\mathrm{Im}\rho^0(t)/[I_L(t)I_S{}^0(t)e^{\alpha z}]^{1/2}. \tag{34}$$

Equation (34) can also be derived from (21).

For an evaluation of $g(\Delta\omega,t)$, we have to solve (30) and (31) in order to obtain $\mathrm{Im}\rho^0(t)$. The solutions of the homogeneous parts of (30) and (31) are obtained by the ansatz

$$\rho^0(t)=\sum_{i=1}^{3}\rho_i e^{\Omega_i t} \tag{35a}$$

and

$$T^0(t)=\sum_{i=1}^{3}T_i e^{\Omega_i t}. \tag{35b}$$

[20] It should be noted that for stimulated thermal Rayleigh scattering the second term with $(z/l)^2$ is essential for calculating the gain at $\omega=0$ (see Refs. 15 and 15a).

The three roots of the characteristic equation have, to a good approximation, the values

$$\Omega_1 = -i\omega - \tfrac{1}{2}\Gamma_R, \tag{36a}$$

$$\Omega_2 = -i\Delta\omega - \tfrac{1}{2}\Gamma_B, \tag{36b}$$

$$\Omega_3 = -2i\omega_B - i\Delta\omega - \tfrac{1}{2}\Gamma_B. \tag{36c}$$

The physical significance of (36) is readily seen when we introduce (35) and (36) into (10). We obtain for the density variation

$$\begin{aligned}\tilde{\rho}(z,t) = \tfrac{1}{2}[&\rho_1 \exp(-\tfrac{1}{2}\Gamma_R t)\exp(-ikz)\\ &+\rho_2 \exp(-\tfrac{1}{2}\Gamma_B t)\exp(i\omega_B t - ikz)\\ &+\rho_3 \exp(-\tfrac{1}{2}\Gamma_B t)\exp(-i\omega_B t + ikz) + \text{c.c.}].\end{aligned} \tag{37}$$

ρ_1 turns out to be the amplitude of a stationary density fluctuation which decays with a time constant $2/\Gamma_R$; according to (19), $2/\Gamma_R$ depends upon the thermal conductivity of the medium and is of the order of 10–100 nsec in most liquids. ρ_2 and ρ_3 are the amplitudes of density waves with the frequency ω_B traveling in the $+z$ and $-z$ directions; ρ_2 generates Stokes and ρ_3 anti-Stokes radiation. Both waves ρ_2 and ρ_3 have decay constants $2/\Gamma_B = 2\tau$, characteristic for acoustic phonons.[21]

Next we discuss the simple case of a constant pump field and a step function like signal pulse; the analytical solution gives good insight into the physical situation.

1. Step Function

In this section, the response of the scattering medium will be investigated, when the input signal at $t=0$ is suddenly turned on, i.e., when

$$\begin{aligned} E_S(0,t) &= 0 \quad \text{for} \quad t<0\\ &= \hat{E}_S{}^0 \quad \text{for} \quad t\geq 0.\end{aligned} \tag{38}$$

The pump light remains constant:

$$E_L(t) = \hat{E}_L. \tag{39}$$

As a particular solution of (30) and (31), we take the steady-state values ρ_{st} and T_{st}, which have been discussed above. The initial conditions are chosen as follows:

$$\rho^0(0) = 0, \quad T^0(0) = 0, \quad \text{and} \quad \dot{\rho}^0(0) = 0. \tag{40}$$

At the beginning of the pulse, the density and temperature disturbance as well as the velocity of the mass element will be zero. [There will be some acceleration $\ddot{\rho}^0(0)$ and temperature rise $\dot{T}^0(0)$.] Solving (30) and (31) for these initial conditions gives the following expressions for the three terms of $\rho^0(t)$:

$$\rho_1 = \rho_{st}\delta/(2\tau'\omega_B), \tag{41a}$$

$$\rho_2 = \rho_{st}[-1+(1-\delta)/(4\tau'\omega_B)], \tag{41b}$$

$$\rho_3 = \rho_{st}(-1-\delta)/(4\tau'\omega_B), \tag{41c}$$

where $\delta = 2(\gamma-1)\gamma^a/(\gamma^a - i\gamma^e)$ and $1/2\tau' = 1/2\tau - i\Delta\omega = -\Omega_2{}^*$. Since $|\delta| \simeq 1$ and $\omega_B|\tau'| \simeq \omega_B/\Gamma_B \gg 1$, we conclude that ρ_1 and ρ_3 are much smaller than ρ_2 and will be neglected. Adding to (35a) the particular steady-state solution ρ_{st}, we obtain for the zeroth order of the density wave

$$\rho^0(t) = \rho_{st}[1 - \exp(-\tfrac{1}{2}\Gamma_B t)\exp(i\Delta\omega t)]. \tag{42}$$

The imaginary part of $\rho^0(t)$ gives, together with (34), the time dependence of the gain factor:

$$g(\Delta\omega,t) = g(\Delta\omega,\infty)\left[1+\exp(-\tfrac{1}{2}\Gamma_B t)\times\left(-\cos\Delta\omega t + \frac{\gamma^e\Delta\omega - \tfrac{1}{2}\gamma^a\Gamma_B}{\tfrac{1}{2}\gamma^e\Gamma_B - \gamma^a\Delta\omega}\sin\Delta\omega t\right)\right], \tag{43}$$

where the steady-state gain factor $g(\Delta\omega,\infty)$ is defined in (25). The result obtained in (43) is interpreted as follows: For $\Delta\omega=0$, i.e., when the frequency of the electromagnetic disturbance $\omega_L - \omega_S$ is exactly equal to the Brillouin frequency of the medium ω_B, then the gain factor approaches monotonously the steady-state value with a time constant equal to twice the phonon lifetime: $(\tfrac{1}{2}\Gamma_B)^{-1} = 2\tau$.

For $\Delta\omega \neq 0$, the gain factor is modulated with the frequency $\Delta\omega = \omega - \omega_B$. This modulation is caused by the frequency mismatch of the electromagnetic perturbation with frequency ω and the sound wave of the medium at ω_B. This phenomenon is again damped with the time constant 2τ.

In Figs. 1(a) and 1(b) curves calculated according to (43) are presented for $\gamma^a = 0$ and for $\gamma^a = \gamma^e$, respectively. The continuous increase of $g(\Delta\omega,t)/g(\infty)$ for $\Delta\omega=0$, and the oscillatory behavior for $\Delta\omega \neq 0$ is quite apparent from the figures. For large values of $2\tau\Delta\omega$, even a change in sign is predicted from Fig. 1(a). For $\gamma^a \neq 0$ the additional contribution of absorptive heating is clearly seen. On the anti-Stokes side ($\Delta\omega<0$), the gain coefficients approach the negative steady-state values which were discussed in connection with (25).

In Sec. III, the observation of transient phenomena (including oscillating amplification) will be reported for liquids and solids.

2. More General Time Dependence

For a more quantitative comparison between theory and experiment we have to consider the special time dependence of the laser pump light and of the incident signal pulse. It is convenient to introduce on the right-hand side of (30) and (31) a function $F(t) \equiv (nc/8\pi) \times E_L{}^*(t) E_S{}^0(t)$. It will be shown below that in many

[21] It has been reported by Enns and Batra that the so-called Rayleigh lifetime $1/\Gamma_R$ is the characteristic time constant for stimulated thermal Brillouin scattering [R. H. Enns and I. P. Batra, Can. J. Phys. 47, 2265 (1969)]. Our results show that ρ_2, responsible for the intense scattering around ω_B, has the characteristic time constant $1/\Gamma_B$.

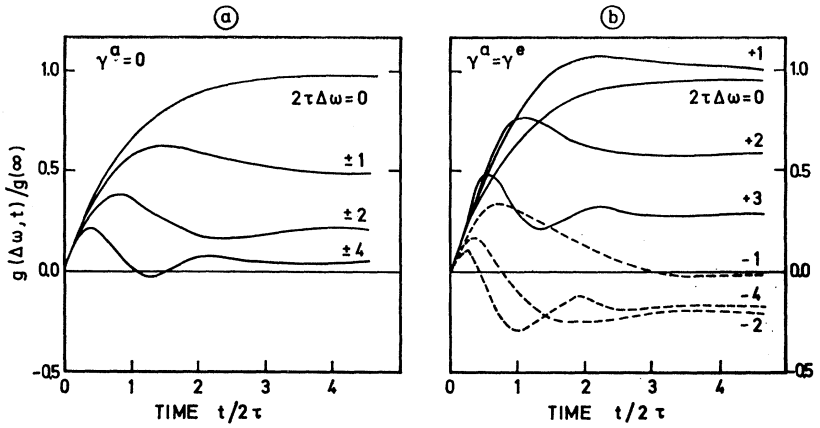

FIG. 1. Trasient gain factor of a step function signal for (a) transparent and (b) absorbing media. The parameter $2\tau\Delta\omega$ represents phonon lifetime τ and mismatch frequency $\Delta\omega$.

experimental situations $F(t)$ is well approximated by functions of the form (52a) or (52b).

The general solutions of the inhomogeneous differential equations (30) and (31) were obtained by the method of the variation of constants; i.e., the roots of the homogeneous problem ρ_i ($i=1,2,3$) in (35a) are considered to be functions of time. First $\rho(t)=\sum_i \rho_i(t)$ is calculated, then, with the help of (32), the first-order increase of the signal amplitude is written as follows:

$$E_S{}^1(t)=\tfrac{1}{4}lE_L(t)e^{-\alpha z/2}\sum_{i=1}^{3} g_i\Gamma_i \times\int_{t_0}^{t} F(t')\exp[\Omega_i{}^*(t-t')]\,dt'. \quad (44)$$

Together with (33) we obtain the (first-order) gain factor

$$g(\omega,t)=\mathrm{Re}\sum_{i=1}^{3} g_i(\tfrac{1}{2}\Gamma_i)\int_{t_0}^{t} F(t')\exp(-\Omega_i{}^*t')dt' \Big/ F(t)\exp(-\Omega_i{}^*t), \quad (45)$$

where

$$g_i=i(\gamma^e\omega_L{}^2h_i)/(nvc^3\rho_0\Gamma_i) \quad (46a)$$

and

$$\Gamma_1=\Gamma_R,\quad \Gamma_2=\Gamma_3=\Gamma_B=1/\tau \quad (46b)$$

and

$$h_1=2\gamma^a,\quad h_2=h_3{}^*=-\gamma^a+i\gamma^e. \quad (46c)$$

The terms for $i=1$ and $i=3$ are related to the Rayleigh and anti-Stokes Brillouin process. The factors $\exp(-\Omega_1{}^*t')$ and $\exp(-\Omega_3{}^*t')$ are rapidly oscillating functions of time with frequencies $\omega\simeq\omega_B$ and $\omega+\omega_B\simeq 2\omega_B$, respectively; the time integrals are negligible for our investigations. For simplicity we restrict our discussion of the Brillouin-Stokes gain to transparent media. With $\Omega_2{}^*=-1/\tau'$, we obtain

$$g(\Delta\omega,t)=g(\infty)\int_{t_0}^{t} F(t')\exp(-t'/2\tau')\,dt' \Big/ 2\tau F(t)\exp(-t/2\tau'). \quad (47)$$

Equation (47) clearly indicates the strong dependence of $g(\Delta\omega,t)$ on $F(t)$, the shape of the laser and the signal pulse. Before a specific example of $F(t)$ is calculated we wish to discuss (47) in general terms by integrating in parts:

$$g(\Delta\omega,t)=g(\infty)\,\mathrm{Re}\tau'/\tau\{[1-2\tau'\dot{F}(t)/F(t) +(2\tau')^2\ddot{F}(t)/F(t)+\cdots]-[1-2\tau'\dot{F}(t_0)/F(t_0) +(2\tau')^2\ddot{F}(t_0)/F(t_0)+\cdots][F(t_0)/F(t)]e^{-t/2\tau} \times(\cos\Delta\omega t-i\sin\Delta\omega t)\}. \quad (48)$$

The following points should be noted:

(i) The first component of (48) contains the negative time derivative $-\dot{F}(t)$ (for small $\Delta\omega$); as a result $g(\Delta\omega,t)$ is depressed during the risetime of signal and pump pulse [$\dot{F}(t)>0$], and enhanced for $\dot{F}(t)<0$. Physically, this means the phonon density does not adjust immediately to the instantaneous light field; the phonon density is too small compared to the steady state during the rise of the signal and pump pulse, but it is too large during the decay time. At the maximum of $F(t)$, where $\dot{F}(t)=0$, the negative value of $\ddot{F}(t)$ still reduces $g(\Delta\omega,t)$ below the steady-state value $g(\Delta\omega,\infty)$. Only for $F(t)=$const does the first term give the steady-state gain factor derived in (25) ($\gamma^a=0$):

$$g(\Delta\omega,\infty)=g(\infty)\,\mathrm{Re}\frac{\tau'}{\tau}=\frac{g(\infty)}{1+(2\Delta\omega/\Gamma_B)^2}. \quad (25')$$

(ii) The second component of (48) tends to decrease exponentially with time, due to the phonon damping factor $\exp(-t/2\tau)$; in addition there is a modulation at the mismatch frequency $\Delta\omega$.

(iii) Developing $F(t')$ in a Taylor series one obtains for times near t_0

$$\lim_{t\to t_0} g(\Delta\omega,t)=g(\infty)t/2\tau(N+1)=At/(N+1), \quad (49)$$

i.e., at the beginning of the amplification the gain factor increases linearly with time and is independent of τ and $\Delta\omega$. N is the order of the first nonvanishing derivative of $F(t)$ at $t=t_0$.

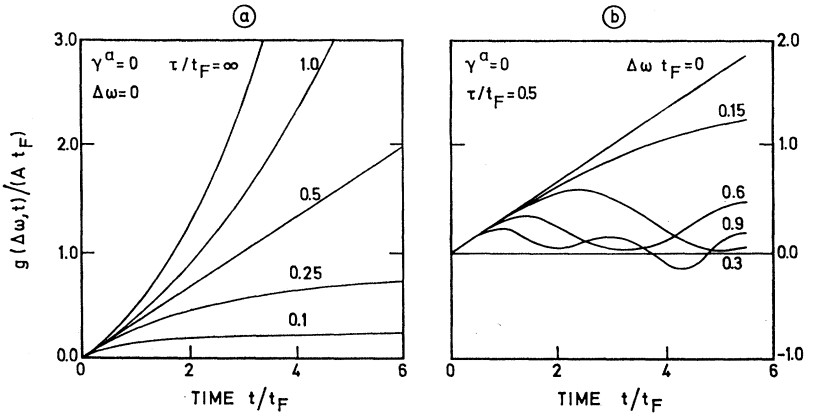

FIG. 2. Transient gain factor of physical pulse (see text) with half-width t_F. (a) Effect of phonon lifetime τ. (b) Effect of frequency mismatch $\Delta\omega$. For comparison with Fig. 1 note: $At_F=g(\infty)$ when $\tau/t_F=0.5$.

(iv) It is readily seen that (48) is a generalized form of (43), which was derived for $I_L=$const, and a step function for the signal field.

3. *Frequency Dependence of* $g(\Delta\omega,t)$

It has been pointed out in connection with the steady-state gain factor [Eq. (25) with $\gamma^a=0$] that values of $g(\Delta\omega,\infty)$ measured as a function of $\Delta\omega$ give the half-width of the Lorentzian frequency profile and in this way the phonon lifetime τ. In practice, we work with light pulses of definite time dependence. Corrections have to be made when τ is deduced from the measured half-width $\Delta\omega_H$. Taking the experimental pulse shape $F(t)$ into account, one obtains from (48)

$$\Delta\omega_H=(1/2\tau)[1+2\tau\dot{F}(t)/F(t) -(2\tau)^2 3\ddot{F}(t)/2F(t)\cdots]. \quad (50)$$

Equation (50) indicates that $\Delta\omega_H$ increases during the rise of the signal and pump light [$\dot{F}(t)>0$] and decreases during the decay. The shorter the pulse $F(t)$, the larger the corrections. Equation (50) will be applied to experimental results in Sec. IV C.

In the literature, the experimental frequency half-width $\Delta\omega_H$ is frequently connected with Γ_B according to the relation

$$\Delta\tilde{\omega}_H=\tfrac{1}{2}\Gamma_B+\tfrac{1}{2}\Gamma_L+\tfrac{1}{2}\Gamma_S, \quad (51)$$

where Γ_L and Γ_S are the half-widths of the amplitude Fourier transforms of the pump and signal pulses, respectively. It should be emphasized that (51) is a rough approximation in most experimental situations. $\Delta\tilde{\omega}_H$ represents a time-averaged value, which is only correct for a special pulse shape not commonly used for I_L and I_S^0.

4. *Specific Cases*

We now turn to the discussion of the function

$$F(t)=\hat{F}(t/t_F)^2 e^{-t/t_F}, \quad (52a)$$

which is a good approximation for the product $E_L^*(t)\times E_S^0(t)$ in a number of our experiments.[22] The parameter t_F, a measure of the pulse duration, is of great importance in the following discussions. Introducing (52a) into (48) we calculate gain factors which are plotted as a function of the normalized time t/t_F in Fig. 2(a) ($\Delta\omega=0$) and Fig. 2(b) ($\Delta\omega\neq0$). The following points should be noted: (a) For $2\tau<t_F$ (τ is short and the pulse duration comparably long) the second term in (48) disappears soon after the beginning of the pulse. A constant value of g is obtained which has the form $g(\infty)\ \mathrm{Re}(\tau'/\tau)[1+2\tau'/t_F]$. Experiments performed under these conditions allow the determination of $g(\Delta\omega,\infty)$ and provide material constants such as τ. (b) For $2\tau\geq t_F$ [τ is long and $F(t)$ decays faster than the phonons] the second term in (48) diverges. At the end of the pulse the phonon density stays high while the light fields go to zero [see (34)]. (c) In Fig. 2(b) the modulation of the gain factor for $\Delta\omega\neq0$ is shown for the case $2\tau=t_F$. Negative values of the gain factor are possible during the transient time. (d) It should be emphasized that all the curves in Figs. 2(a) and 2(b) start linearly with time, independent of τ and $\Delta\omega$; this fact agrees with the prediction of (49).

We have studied the effect of the symmetric function

$$F=\hat{F}\sin^2\pi t/4t_F, \quad (52b)$$

where t_F is chosen in such a way that the maximum of (52b) and (52a) occurs at $t=2t_F$. The gain factors calculated according to (48) are quite similar for both functions (52a) and (52b). We shall return to function (52b) in connection with the slowly rising input signals frequently used for the investigation of liquids (Sec. IV C).

5. *Limits of the SBS Amplifier*

It was shown in Sec. II B *4* that the gain of an amplifier for Brillouin radiation is strongly influenced by the

[22] E_L^* and E_S^0 are proportional to the measured (power of the pumplight)$^{1/2}$, $P_L^{1/2}$, and to the (incident signal power)$^{1/2}$, $P_i^{1/2}$, respectively. Experiments are discussed [e.g., Figs. 5 and 6 (lower traces), and 10] where: (i) the signal rises rapidly and decays slowly; as an approximation we write $P_i(t)\propto(t/t_i)^4\exp(-t/t_i)$; (ii) the signal is only present during the falling part of the pump pulse, i.e., $P_L(t)\propto\exp(-t/t_L)$. Together we obtain (52a) with $1/t_F=1/2t_i+1/2t_L$. F has its maximum at $t=2t_F$,

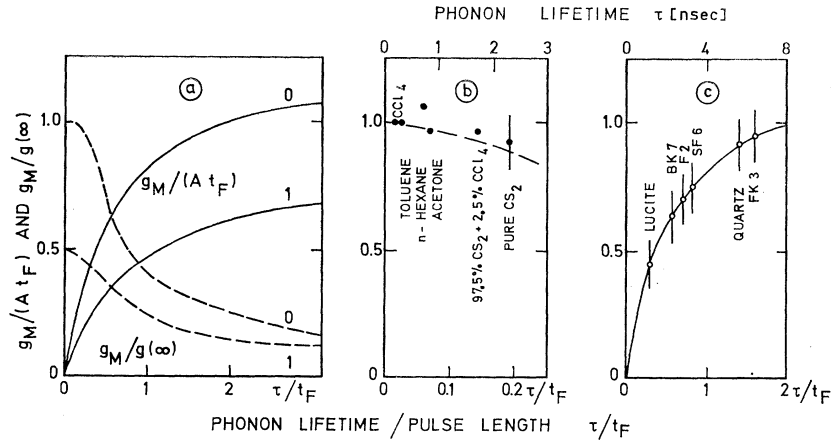

FIG. 3. Gain factor at the maximum of a physical pulse (see text) in units of At_F (solid lines) and $g(\infty)$ (dashed lines). (a) Curves calculated for $2\tau\Delta\omega=0$ and 1. (b) Experimentally determined quasi-steady-state gain factors of six different liquids ($\Delta\omega=0$). Dashed line: calculated ratio $g_M/g(\infty)$. (c) To the determination of the phonon lifetime τ of six solids. Ordinate g_M/At_F; solid line calculated; points added to curve according to experimental values for g_M and t_F.

phonon lifetime and the shape (especially the duration) of the signal and laser pulse. Since it is our aim to determine phonon lifetimes from gain measurements, we investigated the dependence of the gain factor on τ and the form of the light pulses. When the function $F(t)$ has its maximum value, the amplifier gain is determined experimentally with highest accuracy; therefore, we calculate this value g_M as a function of τ. Integrating (52) into parts, we obtain (53) and (54) for the limit of small and large τ

$$\lim_{\tau\to 0} g_M = A\left(\frac{2\tau}{1+2\tau\Delta\omega} + (2\tau)^3\frac{\ddot{F}(t_M)-\ddot{F}(t_0)}{F(t_M)} + \cdots\right), \quad (53)$$

i.e., when the phonon lifetime is very short, the gain factor g_M is, to a good approximation, equal to the steady-state value of (25). For long phonon lifetimes, we find

$$\lim_{\tau\to\infty} g_M = A\left\{\frac{G_0(t_M)}{F(t_M)} - \frac{1}{2\tau}\frac{G_1(t_M)}{F(t_M)} + \left[\left(\frac{1}{2\tau}\right)^2 - \Delta\omega^2\right]\frac{G_2(t_M)}{F(t_M)} + \cdots\right\}, \quad (54)$$

where

$$G_0(t) = \int_{t_0}^{t} F(t')\,dt', \quad G_1 = \int_{t_0}^{t} G_0(t')\,dt', \quad \text{etc.}$$

It is seen from (54) that the value of g_M is mainly determined by the first term and little affected by τ.

We calculated g_M for a variety of condiditions. For the special situation where $F(t)=\hat{F}(t/t_F)^2\exp(-t/t_F)$, calculated values of g_M (in units of At_F) are plotted as a function of τ/t_F (solid lines) in Fig. 3(a). It is seen from this figure that an experimentally determined gain factor g_M would provide for $\tau>t_F$ very poor, and for $\tau>2t_F$ practically no information as to the phonon lifetime. The limiting ($\tau\to\infty$) gain factor $g_M=1.2\,At_F$ is determined by photoelastic parameters only ($2\tau\Delta\omega=0$).

The dashed lines in Fig. 3(a) depict the ratio $g_M(\tau,\Delta\omega)/g(\infty)$ which decreases strongly with increasing τ/t_F; i.e., when the phonon lifetime is larger than the duration of the applied electromagnetic field, the gain at the pulse maximum is substantially reduced compared to the steady-state value $g(\infty)$. The parameters 0 and 1 correspond to the product $2\tau\cdot\Delta\omega$. Curves similar to those, depicted in Fig. 3(a), were obtained using the function (52b).

It should be noted that the theory of transient phenomena presented here is readily extended to other stimulated scattering processes. Very closely connected are the results for stimulated thermal Rayleigh scattering[20] ($\omega_L-\omega_S\simeq 0$) which are derived from the same equations [(5)–(7)].

III. EXPERIMENTAL

The experimental system is depicted schematically in Fig. 4. It consists, essentially, of a giant pulse laser, a generator for backward-traveling Brillouin radiation, and an amplifier cell where the gain of an input signal $P_i(t)$ is measured. The three light pulses, incident laser pulse $P_L(t)$, incident and amplified signal $P_i(t)$ and $P_a(t)$ were measured with the same photocell and oscilloscope using appropriate time delays. The distance laser to amplifier was chosen to be large (18 m) to ensure that Brillouin radiation, back reflected into the laser, did not return during the time of investigation. On the other hand, the distance S of the amplifier to the generator was kept as small as possible to minimize the effect of the frequency drift of the laser[23,24] (see

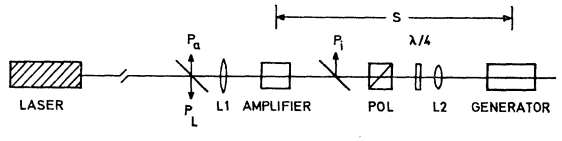

FIG. 4. Schematic of the experimental system. Polarizer (POL) and $\frac{1}{4}\lambda$ plate reduce the backward traveling Brillouin signal.

[23] W. V. Korobkin, A. M. Leontovich, M. N. Poprava, and M. Ya. Shchelev, Zh. Eksperim. i Teor. Fiz. Pis'ma v Redaktsiyu **3**, 301 (1966) [English transl.: Soviet Phys.—JETP Letters **3**, 194 (1966)]; D. J. Bradley, C. Magyar, and M. G. Richardson, Nature **212**, 63 (1966); A. Flamholz and G. J. Wolga, J. Appl. Phys. **39**, 2723 (1968).

[24] D. Pohl, Phys. Letters **26A**, 357 (1968).

below). The polarizer in combination with a $\frac{1}{4}\lambda$ plate served to strongly attenuate the backward-traveling Stokes radiation of the generator (while being transparent to the incident laser light). In this way, ratios $P_i/P_L=10^{-2}$ were achieved and small-signal theory was applicable. The intensity of the pump light in the amplifier was adjusted by the use of lens $L1$ of large focal length.

Some comments should be made concerning our light source. The laser consisted of a 7.5-cm ruby crystal in a spherical cavity; it was Q switched by a saturable dye. Single-mode operation was ensured by the use of an adjustable aperture inside the cavity and a mode-selecting resonant reflector. A careful analysis of the intensity distribution of the output beam indicated that the spot size of the TEM_{00} distribution agreed with the value calculated from the numbers of the laser cavity. Giant pulses with a peak power between 1 and 3 MW and a half-width of approximately 20 nsec were obtained. The finite duration of the laser pulse corresponds to a frequency width of approximately 15 MHz. Recent investigations of our giant pulse ruby laser have shown that, during the course of the pulse, the emission frequency increases by approximately 10 MHz per nsec or 200 MHz per pulse.[24] This frequency drift, although small compared with the laser frequency of 4.3×10^8 MHz, has important consequences for the construction of our experimental system. In order to work with very small frequency differences between the backward-traveling signal pulse and the incoming laser pulse, the distance between oscillator and amplifier has to be kept as small as possible, e.g., for $S=50$ cm, one estimates $\Delta\nu_{\text{drift}}\simeq 50$ MHz. Since the frequency width of the gain profile $\Delta\omega_H\simeq\Gamma_B/2\pi$ [see (25)] is of this order of magnitude for many substances, the distance S has to be substantially below 50 cm in a well-designed experimental system. We succeeded in working with $S=5$ cm, making $\Delta\nu_{\text{drift}}$ a negligibly small value.

Recently, a detailed study of a Brillouin generator was reported by Maier.[8] Brillouin radiation emitted in the backward direction is built up from weak spontaneous scattering to power levels approaching the incoming laser radiation. It was found that the Brillouin radiation has the same frequency drift[24] and a very similar (Gaussian) intensity distribution as the laser beam.[8] There is a distinct onset of intense Brillouin radiation which depends on the gain factor of the medium and the intensity of the incident laser pulse. It is possible, therefore, to "turn on" the generator at the very beginning of the laser pulse or at a later time (e.g., near the maximum of the laser pulse) by changing the focal length of the lens $L2$ in front of the generator from 2 to 12 cm. For a small focal length, the time dependence of the Brillouin radiation follows the laser pulse; we observe a quasi-steady-state amplification in all the liquids investigated. With long focal lengths the Brillouin emission appears later, rising rapidly to large values. The abrupt onset of the Brillouin signal enables us to observe transient phenomena in the amplifier which will be discussed in Sec. IV.

IV. EXPERIMENTAL RESULTS AND DISCUSSION

In this section we wish to present our various experimental investigations and compare them with the theory outlined above. Before entering the discussion some remarks should be made concerning the amplification of real light beams. Our theoretical results were given in terms of intensities, while experimentally, power values are obtained. In our experiments the laser operated in a TEM_{00} mode which gives, for a spherical resonator, a Gaussian intensity distribution

$$I_L(t)=I_L^c(t)\exp(-2r^2/w^2), \tag{55}$$

where the spot size w was experimentally determined (in good agreement with the value calculated from the laser system). Because of the saturation in the generator cell, the intensity distribution of the input signal $I_S(0,t)$ has, to a good approximation, the same distribution as $I_L(t)$. The intensity distribution of the amplified signal $I_S(l,t)$, however, differs from that of the input signal, since the amplification is largest in the center of the beam and decreases with distance from the beam axis:

$$I_S(l,t)=I_S(0,t)\exp[g(t)I_L(t)l]\simeq I_S(0,t)[1+g(t)I_L(t)l]. \tag{56}$$

Integration of $I_L(t)$, $I_S(0,t)$, and $I_S(l,t)$ over the cross section gives $P_L(t)$, $P_i(t)$, and the amplified power $P_a(t)$,

$$P_a(t)\simeq P_i(t)[1+g(t)P_L(t)l/\pi w^2]. \tag{57}$$

Measurement of the pulses $P_L(t)$, $P_i(t)$, and $P_a(t)$ allows the determination of the time-dependent gain factor $g(\Delta\omega,t)$.

A. Time Dependence of the Gain

With laser giant pulses the steady state and transient behavior of the Brillouin gain is demonstrated most vividly with substances having phonon lifetimes of several nsec. In the following experiments CS_2 with $\tau=2.2$ nsec (see below) was chosen. At first our experimental results were qualitatively compared with theory [using the step function (38) for the signal pulse]. The individual pulse shape will be considered later for a quantitative comparison with theory.

1. $\Delta\omega=0$

We begin the discussion with experiments where the frequency of the generator agrees with the frequency of the gain maximum of the amplifier, i.e., the Brillouin generator and amplifier contain the same substance, and the distance S is small enough to make $\Delta\nu_{\text{drift}}$ negligible. In Fig. 5(a), two oscilloscope traces with the three signals P_L, P_i, and P_a are shown. The early start of P_i of trace 1 (which follows P_L during the whole pulse) was

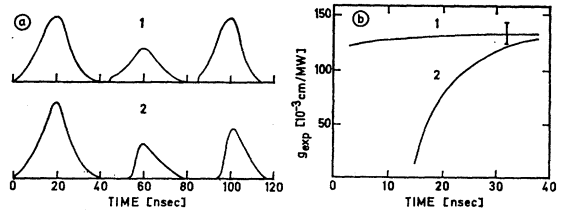

FIG. 5. Amplification of Brillouin light in CS_2 (for $\Delta\omega=0$) (a) Oscilloscope traces of the laser (pump) pulse P_L, the input signal P_i, and the amplified signal P_a. The pulses P_i and P_a are delayed by 40 and 80 nsec, respectively. Trace 1: slowly rising signal P_i. Trace 2: abruptly rising signal P_i. (b) Gain factor determined from the oscilloscope traces of (a).

achieved by the use of a strong focusing lens $L2$ with $f=3$ cm. The gain factor obtained from the data of Fig. 5(a) [see (57)] is presented in Fig. 5(b) (curve 1). g_{expt} is found to be almost constant during the laser pulse.

Second, using a lens $L2$ of $f=12$ cm, a delayed and rather abruptly rising input signal P_i was generated [Fig. 5(a), trace 2). The gain factor shows a transient response with the steady-state value being approached after some nsec [Fig. 5(b), curve 2]. This effect was expected from theory and was predicted in connection with Figs. 1(a) and 2(a).

2. $\Delta\omega\neq 0$

A well-defined frequency mismatch between generator and amplifier was established by using two liquids with slightly different Brillouin shifts ω_B. In Fig. 6(a), trace 1, the amplification of a broad and long input with $\Delta\omega/2\pi=60$ MHz is presented. A comparison with Fig. 5(a) clearly shows the reduced gain due to the frequency mismatch; the gain factor g_{expt} [see Fig. 6(b), curve 1] is accordingly smaller. Gain measurements with varying values of $\Delta\omega$ will be discussed in greater detail in Sec. IV B.

Considerably different results were obtained with faster rising input signals P_i. As expected from the theory [Figs. 1(a) and 2(b)] the gain factor shows an oscillation around the steady-state value [Fig. 5(b), curve 2)]. The experimental gain curve shows good qualitative agreement with Fig. 1(a) ($2\tau\Delta\omega=2$) and with Fig. 2(b) ($\Delta\omega t_F=0.90$).

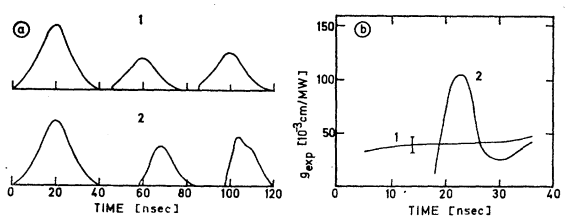

FIG. 6. Amplification of Brillouin light in CS_2 (for $\Delta\omega/2\pi=60$ MHz). (a) Oscilloscope trace 1: slowly rising signal P_i. Trace 2: rapidly rising signal P_i. (b) Gain factors determined from traces depicted in (a).

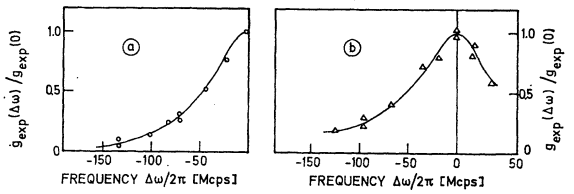

FIG. 7. Experimentally determined frequency dependence of the gain factor. (a) pure CS_2; (b) Mixture of 97.5% CS_2 and 2.5% CCl_4 (by volume).

B. Frequency Dependence of g_{expt} and Phonon Lifetime

It was shown theoretically that the frequency profile of the gain factor g is a direct measure of the phonon lifetime τ. We have measured the frequency dependence of g for a number of liquids. The results obtained with CS_2 will be discussed first.

Experimentally, the input frequency was varied by changing the composition of the liquid in the generator; mixtures of CS_2 and CCl_4 were used in these investigations. In this way, $\omega/2\pi=(\omega_L-\omega_S)/2\pi$ can be tuned from 4300 MHz (corresponding to ω_B of CCl_4) to 5800 MHz (ω_B of CS_2), i.e., a frequency range of 1500 MHz is available using this mixed system.[25]

In Fig. 7(a), the experimentally determined gain factor is plotted as a function of $\Delta\omega/2\pi=(\omega-\omega_B)/2\pi$, where ω_B is the Brillouin frequency of the amplifier cell. The half-width of the experimental gain curve turns out to be $\Delta\omega_H^{\text{expt}}/2\pi=100\pm5$ MHz. To correct for the finite pulse duration we proceeded as follows: Long pulses were used in all the measurements [see, for example, Fig. 5(a)]. The gain factor was evaluated (for every $\Delta\omega$) near the maximum of $F(t)$. The curvature (i.e., $\ddot{F}$) was determined at the maximum of $F(t)$. Finally, (50) was solved for τ. The phonon lifetime of CS_2 obtained from this calculation turns out to be 2.2 ± 0.2 nsec. This value is in good agreement with investigations of the classical Brillouin scattering[26,27] and with calculations of the absorption of hypersonic phonons in CS_2.[27] The sensitivity of our experimental method is demonstrated in Fig. 7(b) where the gain profile of a mixture of 97.5% CS_2 and 2.5% CCl_4 was investigated. The phonon lifetime of this mixture is found to be $\tau=1.9$ nsec.

For decreasing values of τ, the experimental gain profile approaches the Lorentzian curve of the steady-state gain; the correction terms in (50) become accordingly smaller. It should be emphasized that the determination of τ discussed in this section does not require an accurate value of the incident laser intensity; relative gain factors are plotted as a function of $\Delta\omega$. The phonon lifetimes obtained in this way for various liquids are presented in Table I.

[25] F. Barocchi, M. Mancini, and R. Vallauri, Nuovo Cimento **49B**, 233 (1967).
[26] R. Y. Chiao and F. A. Fleury, in Ref. 4, p. 241.
[27] A. Laubereau, W. Englisch, and W. Kaiser, IEEE J. Quantum Electron. **5**, 410 (1969).

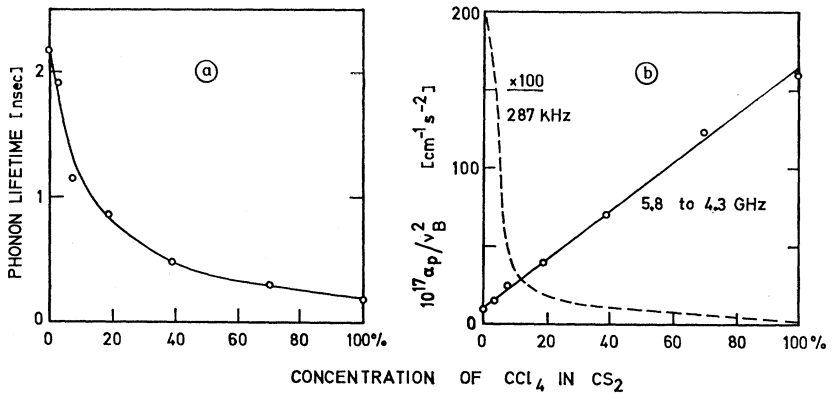

FIG. 8. Experimental results of the mixed system CS_2:CCl_4. (a) Phonon lifetime determined from SBS plotted as a function of the concentration of CCl_4 in CS_2; (b) acoustic absorption α_P at hypersonic frequencies of $\nu \simeq 5 \times 10^9$ Hz and at acoustic frequencies of $\nu \simeq 3 \times 10^6$ Hz (dashed line) (taken from Ref. 30).

C. Quantitative g Value and Phonon Lifetime

The determination of accurate values of g_{expt} requires the knowledge of the absolute laser power P_L [see (57)], i.e., a calibrated photodetector is necessary for these investigations. We have compared our experimental gain factors g_{expt} at $\Delta\omega=0$ with the values $g(\infty)$ calculated from the values of τ in Sec. IV B (Table I). In Fig. 3(b), the ratio $g_{\text{expt}}/g(\infty)$ is plotted as a function of the phonon lifetime τ (upper scale) for six liquids: CS_2, mixture of CS_2 and CCl_4, acetone, n-hexane, toluene, and CCl_4. The ratios are close to unity, i.e., gain coefficients are very near to the steady-state values. The absolute numbers of g_{expt} are listed in Table I.

For a more precise comparison between theoretical and experimental g factor the individual pulse shapes of the light pulses have to be taken into account. In order to be close to the steady-state situation we worked with long pulses, approximated by $\sin^2(\pi t/4t_F)$, and determined g_{expt} again near the maximum of $F(t)$; in this way, we obtained high experimental accuracy and small correction terms in (48). In fact, the theoretical curve [dashed line in Fig. 3(b)] deviates from unity by less than 10%.

Our experimental results suggest that careful measurements of the absolute gain factors provide good numbers of the phonon lifetime; only a single laser pulse is needed in this technique.

Recently, gain measurements were reported of a number of liquids using time-integrating photodetectors.[10] For substances with $\Gamma_B/2\pi < 200$ MHz, the experimental gain factors differ substantially from the calculated values. Our investigations do not show these discrepancies.

D. Phonon Lifetime in Mixed System CS_2:CCl_4

Using the experimental technique outlined in Sec. IV B, various mixtures of CS_2 and CCl_4 were investigated. This system is of special interest since the two liquids have substantially different molecular relaxation frequencies ν_r. For CS_2 the value of $\nu_r = 80$ MHz [28] is far below the Brillouin frequency $\nu_B = \omega_B/2\pi = 5800$ MHz, while for CCl_4 the relaxation frequency $\nu_r = 2400$ MHz [26] is much closer to $\omega_B/2\pi = 4300$ MHz. As a result, the acoustic losses in CCl_4 are expected to be large, being mainly determined by hypersonic relaxation; the phonon lifetime will be correspondingly small. In Fig. 8(a), the phonon lifetime, and in Fig. 8(b) the quantity α_P/ν_B^2 are presented as a function of composition (in volume %) ($\alpha_P/\nu_B^2 = 1/v\tau\nu_B^2$ is characteristic for sound absorption). The strong decrease of τ from 2.2 nsec in CS_2 to 0.25 nsec in CCl_4 and the strong rise of α_P/ν_B^2 is quite apparent from Fig. 8. It is interesting to note that the theoretical curve of Laubereau *et al.*[27] drawn through the measured points in Fig. 8(b) gives an excellent fit to our experimental data. A qualitative agreement exists between the data of Ref. 29 and our results. For comparison we include a damping curve obtained at 287 kHz [30] (dashed line). The result differs completely from our measurement, since the frequency of the ultrasonic wave is well below the relaxation of CS_2 and CCl_4.

E. Brillouin Amplification in Presence of Light Absorption

It was predicted in connection with (25) and (28) that the frequency dependence of the gain factor g is considerably altered when light absorption is added to the medium. We have made such investigations in the amplifier system discussed above (Fig. 4). Our results,

TABLE I. Experimentally determined phonon lifetimes (Sec. IV B): Brillouin linewidths and steady-state gain factors calculated from τ_{expt}. Experimental gain factors (Sec. IV C).

Substance	τ_{expt} (nsec)	$\Gamma_B/2\pi$ (MHz)	$g(\infty)_{\text{calc}}$ (cm/MW)	g_{expt} (cm/MW)
CS_2(pure)	2.2	75	140×10^{-3}	130×10^{-3}
CS_2+2.5% CCl_4	1.9	85	125	120
Acetone	0.9	180	22	20
n-Hexane	0.72	220	23	26
Toluene	0.33	480	15	13
CCl_4	0.25	640	7	6

[28] J. H. Andreas, E. L. Heasell, and J. Lamb, Proc. Phys. Soc. (London) **B69**, 625 (1956).

[29] F. Barocchi, M. Mancini, and R. Vallauri, J. Chem. Phys. **49**, 1935 (1968).

[30] J. Claeys, J. Errera, and H. Sack, Trans. Faraday Soc. **33**, 136 (1937).

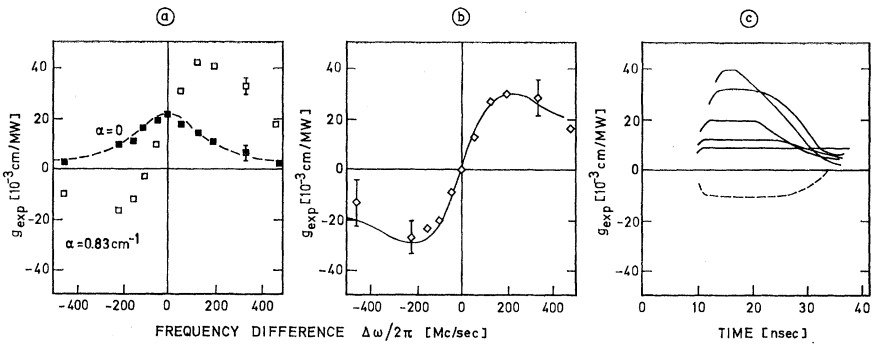

FIG. 9. Brillouin amplification in an absorbing liquid (66% CS_2 and 34% CCl_4). (a) Frequency dependence of the gain factor without (solid squares) and with (open squares) absorption. (b) Difference of gain factors of the two liquids shown in (a). Solid curve gives calculated contribution due to absorption ($\alpha=0.83$ cm^{-1}). (c) Time dependence of the experimental gain factor for various absorption coefficients. Solid lines were measured at $\Delta\omega/2\pi=+200$ MHz, dashed line at $\Delta\omega/2\pi=-200$ MHz.

published in Ref. 14 are summarized as follows: In Fig. 9(a), the frequency profile of a (transparent) mixed liquid consisting of 66% CS_2 and 34% CCl_4 (by volume) is shown by solid square points with a Lorentzian curve drawn through them. A width at half-maximum gain of $\Gamma_B/2\pi=360$ MHz is found. By dissolving a small amount of iodine in this liquid a linear absorption coefficient of $\alpha=0.83$ cm^{-1} was established. The gain profile of the colored liquid was remeasured [open squares in Fig. 9(a)] and a substantial change of the magnitude and the frequency dependence of g was observed. The difference of the gain factors of the two liquids g^a, representing the contribution due to absorption alone, is plotted in Fig. 9(b) versus the frequency $\Delta\omega$. As predicted from theory, g^a is positive for $\Delta\omega>0$ (Stokes or red shift) and negative for $\Delta\omega<0$. A negative gain coefficient [also seen in Fig. 9(a)] indicates that the incident signal P_i is attenuated when passing through the "amplifier" cell; Brillouin photons plus energy from the thermal waves are reconverted into laser photons. It should be noted that the curve drawn through the experimental points in Fig. 9(b) is calculated from theory [Eq. (25)] without fitting parameters. There is excellent agreement between theory and experiment. Experimental investigations of the g dependence on the absorption coefficient again gave agreement with theoretical predictions.[14]

In Fig. 9(c), the time dependence of the gain coefficient during the course of the laser pulse is depicted for liquids with absorption coefficients varying between 0 and 0.83 cm^{-1}. The transparent liquid ($\alpha=0$) shows a constant g value during the whole laser pulse, typical for a quasi-steady-state situation [see Fig. 6(b)]. For α values below 0.85 cm^{-1} the gain coefficients reach a plateau but decrease after several nsec. The values of the plateau were used in Figs. 9(a) and 9(b) and agreed with the steady-state theory. The decay of the gain at later times is not yet completely understood. There is experimental evidence that it results from the competition with another nonlinear phenomenon, the stimulated thermal Rayleigh scattering.[31] Generation of off-axis Rayleigh light was observed to occur frequently in the tilted amplifier cell. Fortunately, thermal Rayleigh scattering has a long time constant, $2/\Gamma_R\simeq 20$ nsec to build up to a power level which disturbs our investigations.[15] In this way the steady-state gain of the thermal Brillouin scattering could be observed during the early part of the laser pulse.

F. Brillouin Amplification in Solids

Gain measurements were made in crystalline quartz, in four different glasses, and in Lucite. With the light pulses used in this investigation the determination of phonon lifetimes is of limited accuracy for two reasons: The phonon lifetime is larger and the gain is smaller than in liquids. As a result, the input signal coming from the generator sets in late and is of short duration.

The transient nature of the gain is clearly seen in these experiments. An estimate of τ was obtained as follows: Generator and amplifier were cut from the same specimen, i.e., $\Delta\omega=0$. The input signal occurred after the peak of the laser pulse, making Eq. (52a) a good approximation for our calculations. The gain g_M was determined at the maximum of the function $F(t)\propto(P_LP_i)^{1/2}$. The parameter A was calculated from the photoelastic data of the sample and t_F was estimated from the shape of $F(t)$. Values of g_M/At_F together with the calculated curve of Fig. 3(a) gave numbers for τ/t_F [see Fig. 3(c)] and allowed, finally, an estimate of the desired phonon lifetime τ. It is readily seen from Fig. 3(c) that the experimental accuracy of g_M is of major importance for large values of τ/t_F.

In Table II, the calculated parameters A and the experimental values g_M^{expt} and t_F^{expt} are listed together with the estimated data for τ; the steady-state gain factor $g(\infty)=A2\tau$ is added for completion. It is interesting to note that the steady-state situation has never

[31] D. H. Rank, C. W. Cho, N. O. Foltz, and T. A. Wiggins, Phys. Rev. Letters **19**, 828 (1967).

TABLE II. Gain factors and estimated phonon lifetimes of glasses and quartz.

Substances	A[a] (cm/MW sec)	t_F^{expt} (nsec)	g_M^{expt} (cm/MW)	τ (nsec)	$g(\infty)$ (cm/MW)
Quartz (x-cut)	0.58×10^6	2.7	1.5×10^{-3}	>4	$>5\times10^{-3}$
Schott glasses:					
FK3	0.45	4.2	1.8	>4	>4
F2	0.69	4.4	2.1	3.5±1.5	5±2
SF6	0.85	3.1	2.0	3.5±1.5	5.5±2
BK7	0.185	3.0	0.35	2±1	0.7±0.3
Lucite	7.0	5.2	17.0	1.5±0.5	20±7

[a] Calculated from literature data: Landolt-Börnstein, *Zahlenwerte und Funktionen* (Springer-Verlag, Berlin, 1962).

been reached in our experiments. The data of Table II show the relatively large τ and small $g(\infty)$ values of the inorganic solids investigated here. The data of glasses cover the range between liquids and crystalline substances such as quartz, where $\tau\simeq5$ nsec. The values of Lucite are close to those of organic liquids.

It has been shown in Sec. II B 5 that for large phonon lifetimes a limiting value of the gain factor g_M exists. As an example, we calculate for X-cut quartz[32]: $g_M(\tau\to\infty)=1.2At_F=1.7\times10^{-3}$ cm/MW; this value has to be compared with the experimental value of $g_M^{\text{expt}}=1.5\times10^{-3}$ cm/MW. Shorter light pulses (i.e., larger τ/t_F values) would provide accurate values of the photoelastic parameter A.

Figure 10 shows for quartz oscilloscope traces for P_L, P_i, and P_a and the experimental gain factor plotted as a function of time. Using different crystallographic directions for the Brillouin generator and amplifier [Fig. 10(a)] a frequency mismatch of $\Delta\omega/2\pi=200$ MHz was established. The drastic transient response of the medium especially the negative g values, should be noted

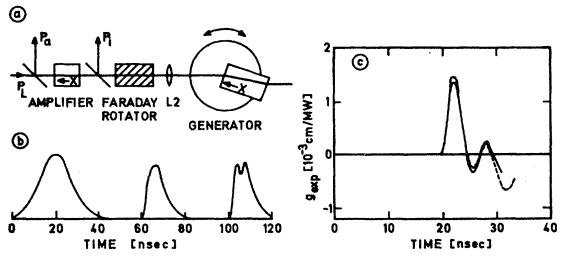

FIG. 10. Amplification of Brillouin light in quartz. (a) Experimental system for the investigation of anisotropic media. The generator can be rotated for variation of the Brillouin frequency. The Faraday rotator (plus a polarizer) attenuate the backward traveling Brillouin signal. (b) Oscilloscope traces of P_L, P_i, and P_a ($\Delta\omega/2\pi=200$ MHz). The pulses P_i and P_a are delayed by 40 and 80 nsec, respectively. (c) Calculated (broken line) and experimentally (solid line) determined gain factor.

[32] The following parameters were used: $c_{11}=8.5\times10^{11}$ g cm^{-1} sec^{-2}, $\rho_0=2.65$ g/cm^3, $n=1.54$, $p_{12}=0.250$ [*American Institute of Physics Handbook* (McGraw-Hill Book Co., New York, 1957), 2nd ed.].

(solid curve). In this experiment, the analytic function for $F(t)$ given in (52a) represents a very good approximation to the experimental situation ($t_F=1.4$ nsec). Values for the gain factor calculated from (48) (dashed curve) are in excellent agreement with the experimental result. The coincidence of the two curves again demonstrates the good description of our experiments by the theory of small signal amplification outlined in Sec. II.

ACKNOWLEDGMENTS

The authors would like to thank I. Reinhold for experimental assistance and Dr. M. Maier and W. Rother for valuable discussions.

APPENDIX

Higher-order contributions of the signal field can be obtained in the same way as (44): For $\gamma^a=0$ we find

$$E_S^{\nu}=\frac{1}{4\nu!}lE_L(t)g(\infty)\Gamma_B\int_{t_0}^{t}E_L^*(t')E_S^{(\nu-1)}(t')\times\exp[\Omega_2^*(t-t')]\,dt'. \quad \text{(A1)}$$

It can be readily seen from (A1) that the $E_S^{\nu}(t)$ do not obey an exponential series law; i.e., in general, $\mathrm{Re}E_S^{\nu}\neq E_S^{0}\frac{1}{2}gI_Ll/\mu!$. The elements $E_S(t)$ of a step function are ($\Delta\omega=0$)

$$E_S(0,t)=[\tfrac{1}{2}g(\infty)I_Ll]^{\nu}E_S^0(t)\times\left[1-e^{-t/2\tau}\sum_{\mu=0}^{\nu-1}\frac{1}{\mu!}\left(\frac{t}{2\mu}\right)^{\mu}\right]. \quad \text{(A2)}$$

The deviation from exponential growth can be considerable for large amplification. It should be noted that it has nothing to do with saturation, and disappears when the steady state is approached. Consequently, the restriction to small amplification, the basis of this analysis, is even more important for the transient than for the steady-state regime.